Available online at www.sciencedirect.com
ScienceDirect
Corrosion Science 49 (2007) 2694–2710
CORROSION SCIENCE
www.elsevier.com/locate/corsci

Biodegradation and corrosion behavior of manganese oxidizer *Bacillus cereus* ACE4 in diesel transporting pipeline

A. Rajasekar [a], T. Ganesh Babu [b], S. Karutha Pandian [b], S. Maruthamuthu [a], N. Palaniswamy [a,*], A. Rajendran [a]

[a] *Microbial corrosion group, Corrosion Protection Division, Central Electrochemical Research Institute, Karaikudi, Tamilnadu 630 006, India*
[b] *Department of Biotechnology, Alagappa University, Karaikudi, India*

Received 8 September 2006; accepted 10 December 2006
Available online 4 January 2007

Abstract

The degradation problem of petroleum products arises since hydrocarbon acts as an excellent food source for a wide variety of microorganisms. Microbial activity leads to unacceptable level of turbidity, corrosion of pipeline and souring of stored product. The present study emphasizes the role of *Bacillus cereus* ACE4 on degradation of diesel and its influence on corrosion of API 5LX steel. A demonstrating bacterial strain ACE4 was isolated from corrosion products and 16S rRNA gene sequence analysis showed that it has more than 99% similarity with *B. cereus*. The biodegradation and corrosion studies revealed that *B. cereus* degraded the aliphatic protons and aromatic protons in diesel and is capable of oxidizing ferrous/manganese into oxides. This is the first report that discloses the involvement of manganese oxidizer *B. cereus* ACE4 on biodegradation of diesel and its influence on corrosion in a tropical country pipeline.

Keywords: A. Steel; B. Polarization; B. SEM; B. X-ray diffraction; C. Microbiological corrosion

* Corresponding author. Tel.: +91 4565 227550; fax: +91 4565 227779.
E-mail address: swamy23@rediffmail.com (N. Palaniswamy).

0010-938X/$ - see front matter © 2006 Elsevier Ltd. All rights reserved.
doi:10.1016/j.corsci.2006.12.004

1. Introduction

Many studies have indicated the importance of microbial tampering of stored hydrocarbon fuels, which leads to the blocking of pipelines and filters, reducing fuel quality and resulting in corrosion of pipeline [1]. Corrosion, the major hallmark of pipeline failure, is the main component affecting the operation and maintenance costs of petroleum industry pipelines [2,3]. It has been anticipated that 40% of all internal pipeline corrosion in the gas industry can be attributed to microbial corrosion [4]. It has been estimated that microbially influenced corrosion (MIC) causes hundreds of millions of dollars in damage to the production, transport, and storage of oil every year in the United States oil industry alone [5].

Generally the major bacteria involved in the microbially influenced corrosion are anaerobic sulfate reducing bacteria (SRB) [6–8]. However, aerobic bacteria and fungi may also participate in the corrosion process [9–11]. The microorganisms influence the corrosion by altering the chemistry at the interface between the metal and the bulk fluid [12,13]. The most extensively studied microorganisms in relation to biocorrosion are the sulfate-reducing bacteria (SRB), whose participation in corrosion was evidenced decades ago [14]. SRB have been repeatedly detected in oil- and gas-producing facilities, as well as in transportation and storage facilities and are most likely the cause for the biocorrosion, souring and biofouling problems that often arise at these sites [6,15–17]. The injection of sulfate-containing seawater into the reservoirs during the secondary recovery of oil favors the proliferation of this type of bacteria. Therefore, most of the research on microbially influenced corrosion has focused on SRB. However, recent studies suggest that SRB need not be present in abundance in all microbial communities responsible for microbially influenced corrosion [18,19]. We recently noticed corrosion in the absence of SRB in diesel and naphtha pipelines [20–22]. Hence, importance of chemolithotrophic bacteria on corrosion is very essential in petroleum product pipeline.

Dickinson and Lewandowski [23], Olesen et al. [24], Dexter and Maruthamuthu et al. [25] and Maruthamuthu et al. [26] concluded that the biomineralized manganese oxides on the stainless steel surface were responsible for the electrochemical behavior of the metal and suggested that the reaction controlling the process was the same as that in alkaline batteries:

$$MnO_2 + H_2O + e^- \rightarrow MnOOH + OH^- \quad E_0' = +382\ \text{mVSCE}$$

Besides Maruthamuthu et al. [21] and Rajasekar et al. [22] noticed the manganese corrosion behavior of oxidizing bacteria in diesel and naphtha pipelines, respectively, and proposed a corrosion mechanism on the role of chemolithotrophic bacteria on API 5LX steel.

Biocorrosion studies involving the use of natural individual species obtained from industrial systems are scarce. However, such studies would better address the actual problem and increase the understanding of the microbial species involved in microbial corrosion and their interactions with metal surfaces which will be the basis for the development of new approaches for the detection, monitoring and control of microbial corrosion in industrial facilities. In the present study, we investigated the role of *Bacillus cereus* ACE4, individual dominant species identified from the corrosion products of a diesel pipeline, on biodegradation of diesel and its influence on the corrosion of API 5LX steel.

2. Materials and methods

2.1. Isolation of bacteria, media composition and culture condition

The corrosion product was collected from a cross-country pipeline in North India, which transports petroleum products such as kerosene, petrol and diesel. This pipeline has intermittent petroleum product delivery cum pressure booting stations at different locations. Severe corrosion and microfouling problems have been observed in the pipeline even though corrosion inhibitor was added. About 300 kg of muck (corrosion product) was removed from a 200 km stretch distance of the pipeline within 30 days due to microbial corrosion [21]. The corrosion product was pushed out of the pipeline by pigs (cylindrical device used for cleaning the interior pipeline). The corrosion products were collected in sterile containers.

Media used throughout for this study were Bushnell Hass medium (BH) consisting of magnesium sulphate – 0.20 gm/l, calcium chloride – 0.02 gm/l, monopotassium phosphate 1 gm/l, dipotassium phosphate – 1 gm/l, ammonium nitrate – 1 gm/l, ferric chloride – 0.05 gm/l, pH 7. For isolation of diesel degraders, 1 gm of corrosion product sample was transferred to 250 ml of Erlenmeyer flask containing 100 ml of BH broth plus diesel ($10\ g\ l^{-1}$) and incubated at 30 °C in a rotatary shaker at 150 rpm until turbid growth was observed. The bacterial culture was diluted and spreaded on BH agar plates containing diesel ($10\ g\ l^{-1}$) as carbon source for selective isolation of diesel degraders. Individual colonies were purified by repeated streaking on BH agar plates containing $10\ g\ l^{-1}$ and a degradation test was conducted with purified isolates.

2.2. Bacterial identification

2.2.1. Biochemical and physiological test

The purified strains were identified by biochemical test according to key described by Bergey's manual of determinative bacteriology [27] and the dominating genus was identified by molecular technique (16s rRNA). These cultures were characterized depending on their morphology, gram staining, spore staining, motility, oxidase, catalase, oxidation fermentation, gas production, ammonia formation, nitrate and nitrite reduction, indole production test, methyl-red and Voges–Proskauer test, citrate and mannitol utilization test, hydrolysis of casein, gelatin, starch, urea and lipid. Ten genera were identified in the corrosion product. The following genera were identified by bio-chemical test: *Bacillus* sp., *Micrococcus* sp., *Vibrio* sp., *Pseudomonas* sp., *Thiobacillus* sp., *Ochrobium* sp., *Xanthobacter* sp., *Gallionella* sp., *Legionella* sp. and *Acinetobacter* sp. The dominating genus among the culturable organisms *Bacillus* sp. has been selected for further study, which was about 50% in pumping station II [28]. Among culturable bacteria, this isolate ACE4 has shown high diesel degradation efficiency when compared to other isolates. Hence, the genus *Bacillus* sp. was selected for further identification by 16s rRNA analysis for biodegradation and corrosion studies.

The strains *B. cereus* ACE4 was checked by leucoberblin blue spot test [29] to find whether this strain accumulate manganese. The pure culture of *B. cereus* ACE4 of individual isolate was streaked repeatedly with an inoculation loop on pre-prepared sterile Mn agar (Hi-media, Mumbai) plates separately. Plates were wrapped in plastic bags to prevent desiccation after few days and incubated at 37 °C for 12 days. Brown colour colonies were observed in the petriplates and scored as "manganese oxidizer" by noticing the appearance

of brown coloration in the colonies. The colonies were picked up and smeared on a filter paper (Whatmann No. 1), using a sterile inoculation loop. Then 0.04% of Leukoberbelin blue (LBB) was added on the filter paper, with the subsequent scrapping of the smear with the inoculation loop. Blue colour was formed after a few minutes on bacterial colonies, which indicated the accumulation and conversion of manganese to manganese-di oxide by manganese oxidizers.

2.2.2. Amplification, cloning and sequencing of 16S rRNA gene

Genomic DNA was extracted according to Ausubel et al. [30]. Amplification of gene encoding for small subunit ribosomal RNA was done using eubacterial 16S rDNA primers (forward primer 5′AGAGTTTGATCCTGGCTCAG3′ (*Escherichia coli* positions 8–27) and reverse primer 5′ACGGCTACCTTGTTACGACTT3′ (*E. coli* positions 1494–1513)) [31]. Polymerase chain reaction (PCR) was performed with a 50-μl reaction mixture containing 2 μl (10 ng) of DNA as the template, each primer at a concentration of 0.5 μM, 1.5 mM $MgCl_2$ and each deoxynucleoside triphosphate at a concentration of 50 μM, as well as 1 μl of Taq polymerase and buffer as recommended by the manufacturer (MBI Fermentas). PCR was carried out with a Mastercycler Personal (eppendorf, Germany) with the following program: initial denaturation at 95 °C for 1 min; 40 cycles of denaturation (1 min at 95 °C), annealing (1 min at 55 °C), and extension (2 min at 72 °C); followed by a final extension at 72 °C for 5 min. The amplified product was purified using GFX™ PCR DNA and Gel Band Purification kit (Amersham Biosciences) and cloned in pTZ57R/T vector according to the manufacturer's instruction (InsT/Aclone™ PCR Product Cloning Kit, MBI Fermentas) and transformants were selected on LB medium containing ampicillin (100 μg/ml) and X-gal (80 μg/ml). Sequencing was carried out using ABI PRISM 310 Genetic Analyzer (PE Applied Biosystems). For sequencing reaction Big Dye Ready Reaction DyeDeoxy Terminator Cycle Sequencing kit (Perkin–Elmer) was employed. The obtained partial 16S rDNA sequence was then submitted to a BLAST [32] search to obtain the best homology sequences.

2.3. Utilization of diesel by B. cereus ACE4

Bacterial culture ACE4 pre-cultured overnight at 30 °C in BH broth medium was transferred to a 250 ml of Erlenmeyer screw capped flask (to prevent loss of volatile diesel hydrocarbon) containing 100 ml of BH plus 10 g l^{-1} of diesel. Cells are grown for 30 days at 30 °C with shaking at 150 rpm, and diesel hydrocarbons remaining in the culture medium were determined. The control (uninoculated) was incubated parallel with experimental system to monitor abiotic losses of the diesel substrate.

2.4. Diesel degradation analyses

At the end of the 30 days of incubation period, the residual diesel was extracted with an equal volume of dichloromethane. Evaporation of solvent was carried out in a water bath at 40 °C. The resultant solution of diesel (1 μl) was analyzed by gas chromatography/mass spectrometry (GC–MS), nuclear magnetic resonance spectroscopy (NMR) and fourier transform infrared spectroscopy (FT-IR).

GC–MS (Thermo Finnigan) has been equipped with a RTX-5 capillary column (30 m long × 0.25 mm internal diameter) and the carrier gas constitutes high pure nitrogen. The

oven temperatures programming was 80–250 °C, with arise of 10 °C/min. To determine the extent of degradation, various hydrocarbon components of diesel was quantified by interpreting the areas of individual peaks and expressing as percentage of degradation relative to the amount of the corresponding peak remaining in the appropriate abiotic control samples. The chromatographic ratios C_{15}/farnesane, C_{17}/pristane and C_{18}/phytane were calculated from the peak heights. NMR analysis (Bruker, 300 mHz) was used to detect the protons of the nuclei in the diesel compound. The sample of diesel was dissolved using deutrated chloroform solvent. Tetra methyl silane (TMS) was used as a reference standard. The FT-IR spectrum (Perkin–Elmer, Nicolet Nexus −470) was taken in the mid IR region of 400–4000 cm^{-1} with 16-scan speed. The samples were mixed with spectroscopically pure KBr in the ratio of 1:100 and the pellets were fixed in the sample holder, and the analysis was carried out. Infrared peaks localized at 2960 cm^{-1} and 2925 cm^{-1} were used to calculate the CH_2/CH_3 ratio (absorbance) and functional group of both aliphatic and aromatic components present in diesel.

2.5. Corrosion studies

2.5.1. Weight loss method

Steel API 5LX (C – 0.29 max., S – 0.05 max., P – 0.04 max., Mn – 1.25 max.) coupons of size 2.5 cm × 2.5 cm were mechanically polished to mirror finish and then degreased using trichloro ethylene. In the present study, 500 ml of diesel with 2% water containing 120 ppm chloride has been used as the control system, while 500 ml diesel with 2% of water containing 120 ppm chloride inoculated with 2 ml of ACE4 inoculum (about 10^8 CFU/ml) was used as the experimental system. After 7 days, the coupons were removed and pickled in pickling solutions, washed in water and dried with air drier. Final weights of the six coupons in each system were taken and the average corrosion rates were calculated. The standard deviation for each system is also presented.

2.5.2. Electrochemical analysis

For electrochemical studies, a mixture of diesel and water (containing 120 ppm chloride ion) in the ratio, 2:1 was made [33]. The API 5LX steel coupons was embedded in araldite with an exposed area of 1.0 cm^2 as a working electrode. In the present study, 75 ml of 1% BH broth (containing 120 ppm chloride) and 150 ml of diesel has been used as the control system, while 75 ml of 1% BH broth (containing 120 ppm chloride) and 150 ml of diesel 500 ml diesel inoculated with 2 ml of inoculum ACE4 about 10^6 CFU/ml was used as the experimental system. The mixtures were stirred vigorously for the periods of 48 and 120 h. After the 4th and 10th day, the coupons were removed and potentiodynamic polarization were carried out by using potentiostate model PGP201 with volta master-1-software. A coupon of API 5LX 1 cm^2 as working electrode, a standard calomel electrode (SCE) and a platinum wire as counter electrode were employed for polarization study. The Tafel polarization curves were obtained by scanning from the open circuit potential towards 200 mV anodically and cathodically. The scan rate was 120 mV/min.

2.5.3. Surface analysis

A computer controlled X-ray diffraction technique (XRD), JEOL Model JDX-8030 was used to scan the corrosion products between 10° and 85° – 2θ with copper Kα radiation (Ni filter) at a rating of 40 kV, 20 mA. The dried corrosion products were collected

and crushed into a fine powder and used for XRD analysis for determining the nature of oxides present in the corrosion product. To verify the adsorption of degraded diesel hydrocarbon products on the metal surface after the electrochemical study in control and inoculated system, the film formed on the metal surface was carefully removed and dried, mixed thoroughly with potassium bromide (KBr) and made as pellets. These pellets are subjected to FT-IR spectra (Perkin–Elmer, Nicolet Nexus −470) to find out the nature of film formed on the surface of the metal coupons. The surface morphological characteristics of the control and experimental coupons API 5LX were observed under scanning electron microscope (SEM) (Hitachi model S-3000 H) at magnification ranging from 50× to 200× operated at accelerating voltage of 25 kV.

3. Results

3.1. Characterization of ACE4

The diesel hydrocarbon biodegradative strain ACE4 was isolated from the corrosion product of diesel transporting pipeline. The preliminary identification of ACE4 by biochemical test indicated that the isolate belonged to the genus *Bacillus* sp. Phenotypic profile of strain ACE4 is shown in Table 1. Fig. 1 shows the formation of blue colour on the pure strain ACE4. LBB spot test confirms the presence of manganese oxide deposition by bacteria. The redox stain (LBB) indicates the accumulation and conversion of manganese by bacterium ACE4. Hence, it can be claimed as *B. cereus* ACE4 is manganese oxidizer.

3.1.1. 16S rRNA gene sequence analysis

Amplification of gene encoding for small subunit ribosomal RNA of ACE 4 was done using eubacterial 16S rDNA primers. The 16S rDNA amplicons derived from ACE4 was cloned in pTZ57R/T vector. The recombinant plasmid (pACE4, harboring 16S rDNA

Table 1
Phenotypic profile of strain ACE4

Positive for biochemical test	Negative for biochemical test
Catalase	Indole production
Cytochrome oxidase	Starch hydrolysis
Voges–Proskauer	Utilization of
Reduction of nitrate	Sucrose, galactose, adonitol, arabinose
Gelatinase, casein hydrolysis	Cellobiose, inulin, sorbitol, mannose
Utilization of D-glucose, fructose, maltose, salicin, trehalose, xylose	Lactose, melibiose, raffinose, rhamnose Mannitol, inositol

Fig. 1. Detection of manganese accumulation by *Bacillus cereus* ACE4 using leucoberblin blue (LBB) spot test (duplicate samples).

insert) was partially sequenced. The sequence obtained was matched with the previously published sequences available in NCBI (National Centre for Biological Information) using BLAST. Sequence alignment and comparison revealed more than 99% similarity with *B. cereus*. The nucleotide sequence data have been deposited in GenBank under accession number AY912105.

3.2. Degradation analyses

Biodegradation of diesel hydrocarbon by *B. cereus* ACE4 was confirmed by gas-chromatography–mass spectroscopy (GC–MS) analyses, nuclear magnetic resonance spectroscopy (NMR) and fourier transform infrared spectroscopy (FT-IR). No evaporation of diesel fuel from the screw capped flasks was observed throughout the experiments. From the GC–MS analysis, it was observed that the uninoculated system (diesel) consists of mixture of hydrocarbon from C_{10} to C_{20} consist of *n*-alkanes, branched alkanes (Pristane, Phytane) together with aromatic hydrocarbon having naphthalene derivatives and substituted naphthalene (Fig. 2a). Inoculated system of *B. cereus* ACE4 degraded almost all the *n*-alkanes (C_{10}–C_{20}) and many of the branched alkanes found in diesel (Fig. 2b). Overall, the bacterium is capable of utilizing a broad range of alkanes and aliphatic components present in diesel.

The NMR spectra (Fig. 3a) of control system (pure diesel) show major peaks at 0–3 chemical shifts (δ). It indicates the presence of aliphatic protons. The other peaks at 6–7 chemical shifts (δ) indicates the presence of benzene ring. In the ACE4 inoculated system the new peaks obtained in the range between 3 and 5 chemical shifts (δ), indicates the addition of oxygen with carbon atoms (–O–CH_2–). In the presence of *B. cereus*, aliphatic proton (0–3 chemical shifts (δ)) peaks and benzene peaks (6–7 chemical shifts (δ)) disappeared because of biodegradation (Fig. 3b). From this it is evident that aliphatic protons (CH_2–CH_2) are completely broken by bacterial species, and converted as (–O–CH_2) group. Further, it is certain that the strain is involved in the utilization of both aliphatic and aromatic hydrocarbons present in the diesel.

In Fig. 4a, the FT-IR spectra of control system (uninoculated system) shows the characteristic band at 2952 cm^{-1}, 2920 cm^{-1} and 2852 cm^{-1} (C–H aliphatic stretch); 1459 cm^{-1} and 1376 cm^{-1} (CH def for methyl group), 722 cm^{-1}, 743 cm^{-1}, 699 cm^{-1} (meta disubtituted benzene) and 873 cm^{-1}, 810 cm^{-1} (disubstituted benzene). FT-IR spectra of experimental system (inoculated with ACE4) shows the characteristic bands (Fig. 4b) at 2853 cm^{-1} and 2904 cm^{-1} (C– H aliphatic stretch); free OH peaks at 3315 cm^{-1}, 1632 cm^{-1} (C=C stretch); 1461 cm^{-1} and 1376 cm^{-1} (CH aliphatic stretch for methyl groups). A new peak at 1632 cm^{-1} appeared which indicates a carbonyl group (C=O) stretch. The absence of aromatic nuclei peaks at 847 cm^{-1}, 809 cm^{-1}, 873 cm^{-1}, 722 cm^{-1}, and 743 cm^{-1} (Mono and di substituted benzene) indicates the utilization of aromatic hydrocarbon. The intensity of C–H aliphatic stretches at 2954 cm^{-1}, 2923 cm^{-1} and 2854 cm^{-1} decreased. It points out the aliphatic hydrocarbon degradation (Fig. 4b). After 30 days of growth in BH broth containing 1% diesel, *B. cereus* was capable of utilizing both the aliphatic and aromatic hydrocarbon present in diesel.

3.3. Corrosion studies

3.3.1. Weight loss method

In the control system (uninocualted), the weight loss was 30.4 mg whereas in the presence of *B. cereus* ACE4 the weight loss was 57.5 mg (Table 2).

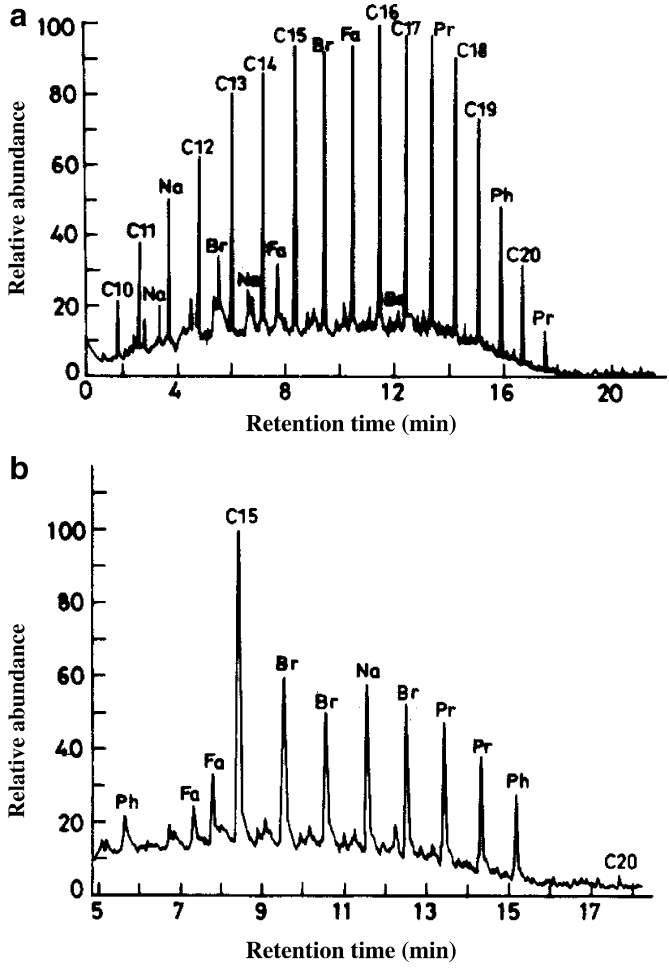

Fig. 2. GC–MS profiles of diesel oil extracted from the aqueous phase of BH medium after 30 days of incubation at 30 °C with and without inoculation with *Bacillus cereus* ACE4. (a) GC–MS profiles of abiotic control (uninoculated). (b) Inoculated with ACE4. C10–C21, *n*-alkanes (numbers designate the number of C atoms); Br, branched alkanes; Na, substituted naphthalenes; Pr, pristane; Ph, phytane. The alkane, naphthalene, phytane, and pristane peaks were identified by comparison of their retention times and mass spectra with authentic standards.

3.3.2. Electrochemical analysis

Fig. 5 shows the polarization curve for steel API 5LX in diesel–water system in presence/absence of bacteria on 4th and 10th day. On 4th day, the corrosion current for control system is 4.025×10^{-5} A/cm^2 while in presence of bacteria the current is 2.62×10^{-5} A/cm^2 (Table 3). The corrosion potential for control system is −711 mV vs. SCE and in presence of bacteria the potential value is −879 mV vs. SCE at 4th day. On the 10th day, the corrosion current for control and experimental system is 1.085×10^{-5} A/cm^2 and 3.666×10^{-6} A/cm^2, respectively. The nature of the curves for the 4th day, both anodic and cathodic curves shifted to left side, which indicates that the bacterium ACE4 suppresses both anodic and cathodic reactions. It may be due to the production of metabolic activity of ACE4 by

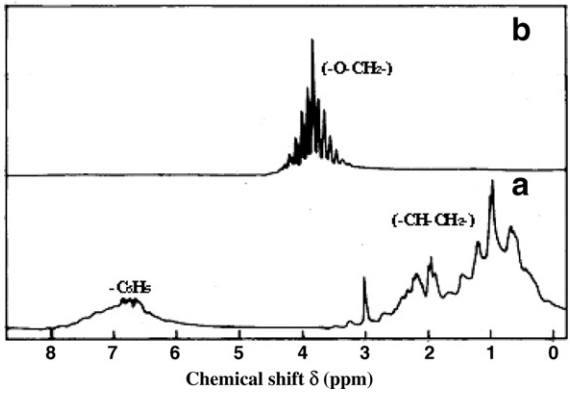

Fig. 3. NMR Spectrum of diesel and diesel inoculated with ACE4. (a) NMR spectrum of diesel and (b) NMR spectrum of diesel inoculated with ACE4.

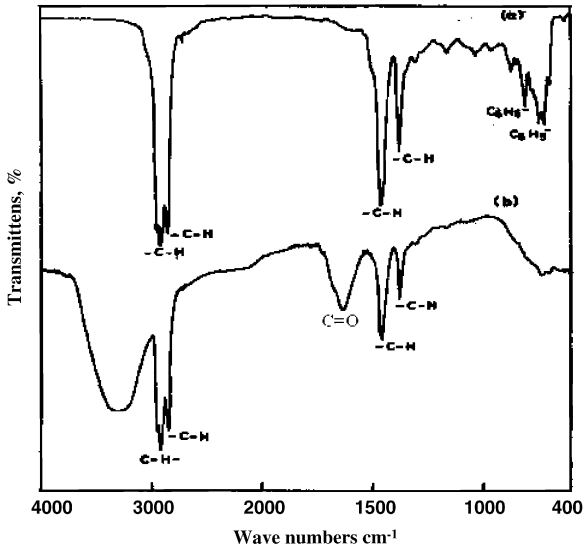

Fig. 4. Fourier-Transform Infrared Spectrum of diesel and diesel inoculated with *Bacillus cereus* ACE4. (a) FT-IR spectrum of diesel and (b) FT-IR spectrum of diesel inoculated with ACE4.

Table 2
Corrosion rate of steel API 5LX

System	Weight loss (mg)	Corrosion rate (mm/y)
Control system: 500 ml diesel + 2% water (120 ppm chloride)	30.4 ± 2.2	0.1059
Experimental system: 500 ml diesel + 2% water (120 ppm chloride) + *Bacillus cereus* ACE4	57.5 ± 1.1	0.2003

phosphate based compounds and oxygen consumption in the electrolyte. On 10th day, the potential goes to negative side from −601 mV to −717 mV vs. SCE. In control, slight passiv-

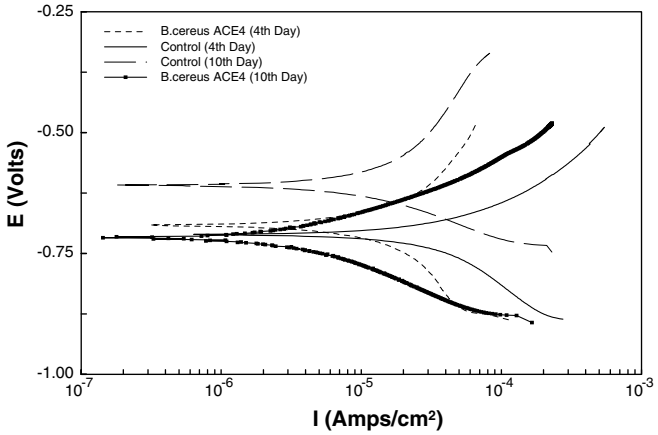

Fig. 5. Polarization curves for API 5LX in diesel water system in presence/absence of ACE2 at different periods.

Table 3
Polarization study for API 5LX in presence/absence of ACE4

Systems	Immersion periods (days)	E_{corr} (mV)	b_a (mV/decade)	b_c (mV/decade)	I_{corr} (A/cm^2)
Control system					
75 ml of 1% BH broth	4	−711	158	206	4.025×10^{-5}
(containing 120 ppm chloride) and 150 ml of diesel	10	−601	283	94	1.085×10^{-5}
Experimental system					
75 ml of 1% BH broth	4	−879	330	278	2.62×10^{-5}
(containing 120 ppm chloride) and 150 ml of diesel and inoculated with 2 ml of inoculum ACE4 about 10^6 CFU/ml	10	−717	106	121	3.666×10^{-6}

ation can be noticed. At the same time the anodic curve shifted to right side and enhances the anodic current on 10th day where the Tafel corrosion current is lower in bacterial system. It can be assumed that though i_{corr} does not show any significant variation on 10th day the formation of pit on the metal sample may be the reason for the higher anodic current.

3.4. Surface analysis

Fig. 6a and b present the details of XRD data corresponding to the phases present in the corrosion product sample collected from control and experimental systems. α-Iron oxide hydroxide (α-FeO(OH)), ferrous hydroxide ($Fe(OH)_2$) and ferrous chloride ($FeCl_2$) were observed in the control system (Fig. 6a). More intensity peaks of α-ferric oxide (Fe_2O_3), α-iron oxide hydroxide α-FeO(OH), ferric chloride ($FeCl_3$), ferrous hydroxide ($Fe(OH)_2$) and λ-manganese di oxide (λ-MnO_2) were noticed in the experimental system (Fig. 6b). XRD results reveal the presence of ferric oxides (Fe_2O_3) and manganese oxides (λ-MnO_2) indicating the role of *B. cereus* ACE4 on manganese/iron deposition during the formation of corrosion product and accelerate the microbial corrosion directly on the pipeline. The confirmatory test by leucoberblin blue also supports the XRD observation.

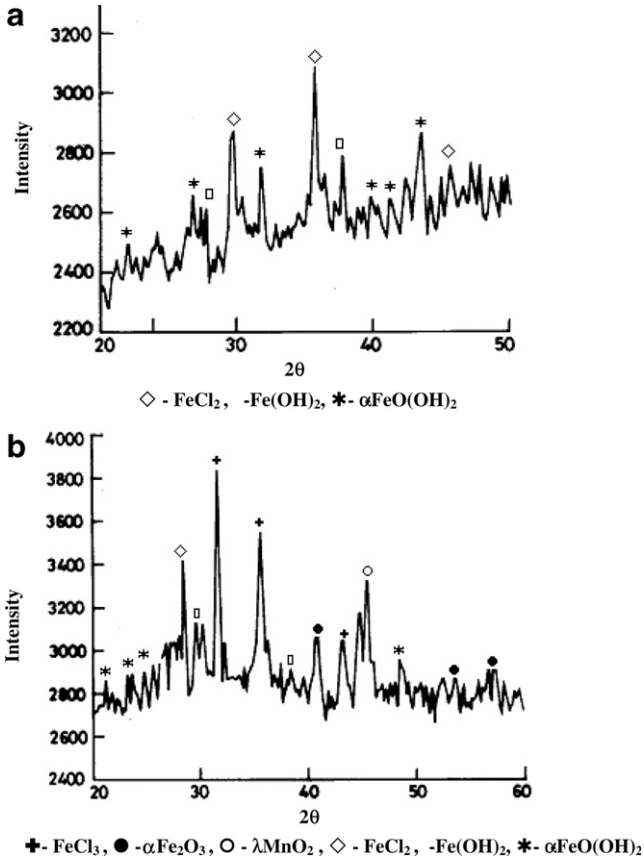

Fig. 6. Analysis of corrosion product on steel API 5LX exposed to ACE4 by XRD analysis. (a) XRD pattern of corrosion product – control system. (b) XRD pattern of corrosion product of experimental system, inoculated with ACE4.

Since it is a redox strain, it turns blue colour while adding Leucoberblin blue in the pure culture of bacteria (Fig. 1).

The FT-IR spectrum of the surface film on the metal surface after polarization study in presence/absence of ACE4 is shown in Fig. 7. In control system Fig. 7a (uninoculated) the peak at 1023 cm^{-1} is due to the presence of –C–O– stretch for –C–O–C– group. A peak at 668 cm^{-1} indicates the presence of FeO stretch and the peak at 472 cm^{-1} due to C–Cl bond. In presence of bacteria (Fig. 7b) the peaks are noted in the range of 2921 and 2852 cm^{-1}, which are assigned to the presence of –CH– aliphatic stretching for aliphatic hydrocarbon present in the diesel. The peak at 1651, 1559, 1459 and 1541 cm^{-1} are due to COO^{-} (carboxylate anion). This peak may be formed due to the bacterial exopolymer secretion. A peak at 1021 cm^{-1} indicates the presence of stretching for –C–O– stretch for –C–O–C– group. A peak at 749 cm^{-1} indicates the presence of FeO and the high intensity of this peak indicates more iron oxide formation by the ACE4. The peak at 472 cm^{-1} is due to C–Cl bond.

The surface morphological characteristics of the control and experimental steel API 5LX coupons were observed under scanning electron microscope. Fig. 8a–c show the

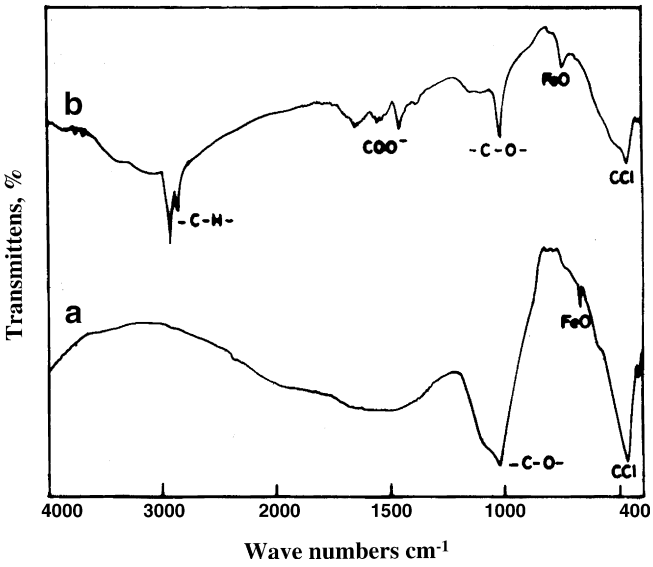

Fig. 7. Fig. 5. Surface film on the metal surface in presence/absence of ACE4 (a) Control (b) ACE4.

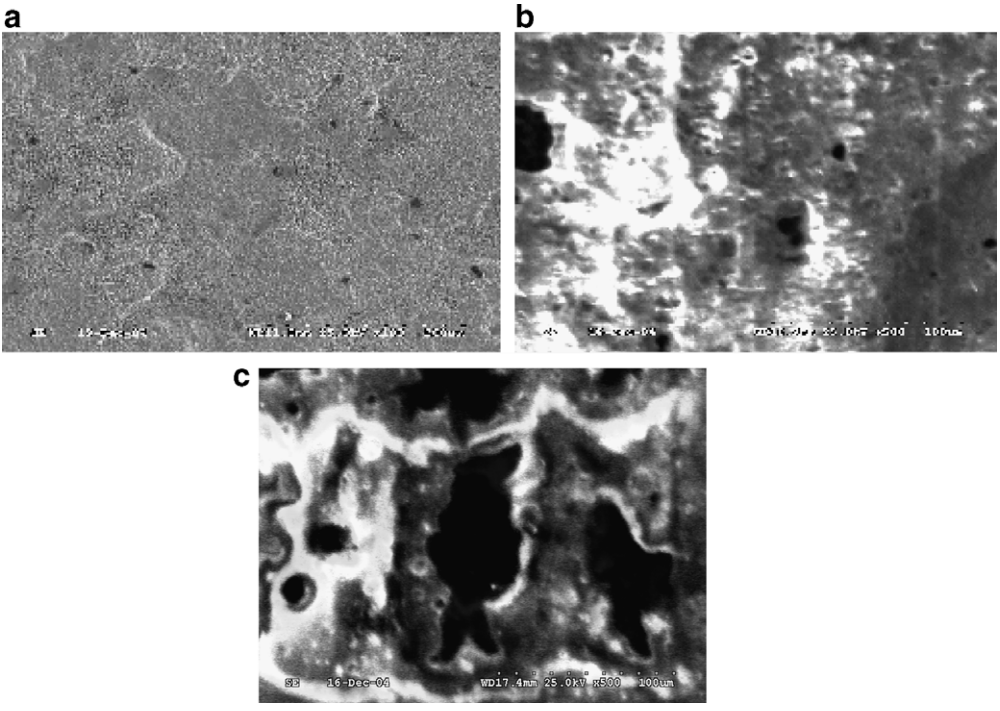

Fig. 8. Scanning electron microscopy (SEM) indicating that the bacterial strain ACE4 is capable of influencing corrosion. (a) SEM of API 5LX (control system) (b) SEM micrograph of steel API 5LX surface, showing localized attack, following exposure to ACE4. (c) Closer view of the pit on the surface of API 5LX steel.

SEM micrograph of the API 5LX steel coupons after 7 days of exposure in the bacteria inoculated system and uninoculated system after removing the corrosion products and biofilm. Uniform corrosion was noticed in control system (Fig. 8a) whereas in experimental system severe pitting attacks were observed over the surface of steel (Fig. 8b). Fig. 8c shows the magnification of the pit and the size of the pit was about 200 μm in diameters.

4. Discussion

Microbiologically influenced corrosion is one of the well documented phenomena in corrosion, which causes deleterious effect on petroleum product pipeline, storage tanks and various industries. The diverse group of bacteria and fungi has been reported in hydrocarbon degradation [34–39]. In oil pipelines, water can also stratify at the bottom of line if the velocity is less than that required to drain water and sweep it through the pipeline system. Liquids (hydrocarbon) stratify along the bottom of the pipe, with water forming a separate layer beneath the liquids where hydrocarbon degradation occurs at the interface easily by microbes [21]. Hence, the role of bacteria on degradation and corrosion is an important area in petroleum product pipelines. However, there are only few reports available on involvement of individual bacterial species on diesel degradation and corrosion. This is the first study that enlightens the role of manganese oxidizer *B. cereus* ACE4 on biodegradation and corrosion process in a tropical country pipeline. Previous microbiological studies have concluded that SRB play a major role in microbially influenced corrosion [4,6,8,40,41]. Phylogenetic characterization and environmental scanning microscopy analysis of corrosive consortium of sour gas pipeline revealed the low abundance of SRB in sour gas pipeline [18,19]. These studies demonstrate that SRB need not be present in abundance in all microbial communities responsible for microbially influenced corrosion in petroleum industry. The bacterial strain ACE4 was isolated from diesel transporting pipeline where SRB could not be noticed in the pipeline. It can be explained that flow velocity may create uniform distribution of oxygen, which may suppress the distribution of SRB [19]. Hence, an investigation on the role of dominating facultative anaerobic species and manganese oxidizer *B. cereus* ACE4 on corrosion process is worthwhile in the diesel pipeline in the absence of SRB.

16S rRNA gene sequence analysis of the demonstrating bacterial strain ACE4 isolated from the corrosion product showed close similarity (about 99%) with *B. cereus*. This isolate has the capacity to degrade the diesel hydrocarbon as well as to accelerate the corrosion process. The ACE4 degrade both aliphatic and aromatic hydrocarbon present in the diesel. In the present study, FT-IR reveals the absence of aromatic nuclei peaks at 847 cm^{-1}, 809 cm^{-1}, 872 cm^{-1}, 722 cm^{-1}, and 743 cm^{-1} (Mono and di substituted benzene) during degradation process (Fig. 3b). GC–MS results reveal that bacterium ACE4 utilized almost all the *n*-alkanes (–CH_2–CH_2–) and moderately attacked the branched alkanes including phytane, pristane and naphthalene derivatives (Fig. 1b) which is a common feature of many other hydrocarbon degraders [42,43]. It was reported that benzene is converted to catechol (an orthohydroxy phenol) and fission occurs between the carbon atoms being two hydroxyl groups to form *cis–cis*-muconic acid which is then converted into 3-oxoadipic acid via the action of a catechol 1, 2-oxygenase [44]. During degradation *n*-alkanes were converted into (–O–CH_2–) which was identified in NMR studies (Fig. 2b). The conversion was due to hydrogen consumption and the very rapid addition of oxygen in the

place of hydrogen by bacterial metabolic activity [20,21]. Overall, the bacterium is capable of utilizing a broad range of alkanes and aliphatic components present in diesel.

Weight loss study indicates the bacterial corrosion on the metal surface. The electrochemical study carriedout at the 4th day indicates the bacterium ACE4 suppress both anodic and cathodic reaction where as at 10th day, ACE4 accelerates the anodic reaction and reduces the cathodic reaction. It can be explained that due to the adsorption of degraded products with Fe^{2+} (organometallic components) on the metal surface, it may be reduce the current flow on the metal surface which does not show significant difference in i_{corr} values [45]. Leucoberblin blue test (Fig. 1) confirms that the ACE4 is able to oxidize the manganese present in the metal into oxides. Hence, it can be concluded that this strain ACE4 is also capable of producing oxides of iron and manganese [46,47]. The enzymatic processes are classified by three groups of organisms: (i) Those which oxidize dissolved Mn^{2+} and (ii) organisms which oxidize Mn^{2+} prebound to certain solids. Both groups utilize oxygen as the terminal electron acceptor and certain organisms may derive useful energy from this reaction. Group (iii) organisms oxidize dissolved Mn^{2+} by the metabolic H_2O_2 via catalase. All manganese oxidizing bacteria known so far are aerobes and the oxidation of Mn^{2+} is often closely related to the oxidation of Fe^{2+}. The most manganese oxidizing bacteria form manganese oxides in the cell envelope or completely outside the cell, we may speculate about the possibility of a direct coupling of a Mn redox enzyme to a metal substrate. If this is the case, we could expect anodic potential shifts of passive metals without massive (observable) formation of MnO_2. A similar situation arises if we assume that the manganese oxide, produced by cells on the surface of a metal is reduced immediately by corrosion currents when it is formed. This could mean large corrosion rates for non-passivating metals such as carbon steel [48].

Since ferric/manganese has high affinity to oxygen, it takes oxygen from (–O–CH_2–) and encourages the formation of ferric/manganese oxides and accelerates the corrosion and again (–CH_2–CH_2–) was formed. It can be explained that since electrons are needed continuously for ACE4 for its activity, it converts the Fe^{2+} to Fe^{3+}, Mn^{2+} to Mn^{3+} and forms ferric oxides (Fe_2O_3) and manganese oxides (MnO_2) by continuous addition of oxygen. This bacterium is capable of oxidizing manganous ions to manganic ions with concomitant deposition of manganese di oxide and dense accumulation on metal surface and promotes corrosion. Jones et al. [49] suggests that the insoluble product is a mixture of ferric oxide (FeO_3) and ferric hydroxide ($Fe(OH)_3$), in which an approximate formula is $FeO(OH)_n$. The ferric ions are not precipitated completely, especially in the acidic crevice regions. Ferric ions in solution serve as highly oxidizing species and tend to accelerate corrosion. Moreover, in waters containing chloride ions, iron-oxidizing bacteria may be directly involved in the production of ferric chloride which is an extremely corrosive substance that can concentrate under nodules [50,51]. Chloride ions can migrate into a crevice location by neutralizing the increased charge via anodic dissolution and then combine with the oxidation of ferrous and manganous ions to ferric and manganic ions by ACE4 and it is observed in the corrosion products (Fig. 4b).

In the present study, though complex is formed on the metal surface, due to the degradation of diesel at the interface act as humic substances resulting in the high supply of electron to the metal surface and accelerates the corrosion. It can be inferred that the degraded diesel hydrocarbon coordinated with Fe^{2+} through the –C–O–C– and carbonyl oxygen resulting in the formation of Fe^{2+} hydrocarbon complex on the metal surface. The corrosion damage observed on the steel surface exposed to the isolate ACE4 was more severe

pitting attack on the steel (Fig. 8b and c) than the damage observed under control system (Fig. 8a). It is observed that the cavities created by bacterium, bioleached the tunnels through the iron/manganese oxides deposit as a result of microbiologically influenced corrosion [52].

Based on the overall result we put forward the hypothesis. It can be concluded that the degraded organic compounds in diesel accelerate the formation of ferric oxide, subsequently the ACE4 encourages the corrosion process by formation of Fe_2O_3. Degraded carbon (diesel) acts as a good nutrient for bacteria, which increases the proliferation of bacteria on the steel and determine the nature of degradation and corrosion.

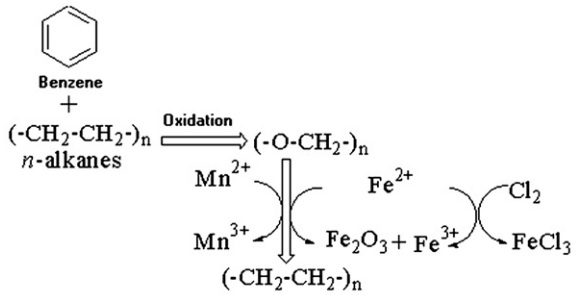

5. Summary

In summary, this studies provided the first look on the role of *B. cereus* ACE4 in biodegradation of diesel and in the corrosion process in a tropical country pipeline. It can be concluded that *B. cereus* ACE4 is one of the most proficient diesel degrader among the culturable organisms isolated from corrosion product collected from diesel transporting pipeline. It is a major aromatic and aliphatic degrader that breaks the benzene ring and aliphatic (–O–CH_2–) chain allowing inclusion of oxygen and accelerating the corrosion by ferric oxide formation in diesel environment. The presence of manganese and ferric oxides in the corrosion products indicated that *B. cereus* ACE4 is capable of converting the ferric and manganese on metal into oxides and accelerates severe pitting attack on the surface of steel API 5LX. This investigation clearly indicates the possibility of break down of diesel by *B. cereus* ACE4 at the stagnant areas of the pipelines. Eventhough, these bacteria could be useful in the bioremediation of diesel polluted habitat, their presence in diesel pipeline and transportation facilities would lead to the reduction in the quality of diesel and in turn economic loss.

Acknowledgements

We thank CSIR, India, for the Senior Research fellowship (SRF) granted to one of the authors (A. Rajasekar). The author thanks Shri. N. Muthukumar, SRF, Central Electrochemical Research Institute, (CECRI), Karaikudi for his help in taking FT-IR and NMR and related discussions. Grateful to Dr. S. Mohanan, Dr. P. Subramanian and Dr. S. Ponmariappan, CECRI, karaikudi, for their help in field collection in petroleum product pipeline, North West, India. The authors also thank Dr. K. Pitchumani and Vijayakumar School of Chemistry, Madurai Kamaraj University, Madurai for their help in GC–MS

analysis. N.A. Choudhury, Solid State and Structural Chemistry Unit, Indian Institute of Science, Bangalore for XRD ananlysis.

References

[1] C.C. Gaylarde, F.M. Bento, J. Kelley, Rev. Microbiol. 30 (1999) 01.
[2] E. Buck, G.C. Maddux, R.L. Sullivan, Internal corrosion cost impact study – United States natural gas exploration and production industry. GRI-96/0056 document No. 96-1466. Gas Research Institute, Des Plaines, III, 1996.
[3] G.H. Koch, M.P.H. Brongers, N.G. Thompson, Y.P. Virmani, J.H. Payer, Corrosion costs and preservative strategies in the United States. FHWA-RD-01-156. (Online) Federal Highway Administration, Washington, DC, <http://corrosioncost.com>, 2001.
[4] J.W. Graves, E.H. Sullivan, Mater. Prot. 5 (1996) 33.
[5] J.W. Costerton, J. Boivin, Microbially influenced corrosion, in: M.W. Mittelman, G.G. Geesey (Eds.), Biological Fouling of Industrial Water Systems. A Problem Solving Approach, Water Micro Associates, San Diego, CA, 1987, pp. 56–76.
[6] W.A. Hamilton, Annu. Rev. Microbiol. 39 (1985) 195.
[7] D.H. Pope, R.M. Pope, Guide for the monitoring and treatment of microbiologically influenced corrosion in the natural gas industry, GRI report GRI-96/0488. Gas Research Institute, Des Plaines, III, 1998.
[8] G.J.K. Voordouw, T.R. Voordouw, J. Jack, P. Foght, M. Fedorak, D.W.S. Westlake, Appl. Environ. Microbiol. 58 (1992) 3542.
[9] F. M Bento, C.C. Gaylarde, Int. Biodeterior. Biodeg. 47 (2001) 107–112.
[10] J.L. Shennan, Control of microbial contamination of fuels in storage, in: D.R. Houghton, R.N. Smith, H.O.W. Eggins (Eds.), Biodeterioration, Elsevier, Barking, 1988, pp. 248–254.
[11] H.A. Videla, W.G. Characklis, Int. Biodeterior. Biodeg. 29 (1992) 195.
[12] D.A. Jones, P.S. Amy, Corrosion 58 (2002) 638.
[13] B. Little, R. Ray, Corrosion 58 (2002) 424.
[14] C.A.H. Von Wolzogen Kuhr, I.S. Vander Klugt Water, Water 18 (1934) 147.
[15] E.D., Burger, Method for inhibiting microbiologically influenced corrosion. US Patent 5,753,180, 1998.
[16] E.P. Rozanova, G.A. Dubinina, E.V. Lebedeva, L.A. Suntsova, V.M. Lipovskich, N.N. Tsvetkov, Microbiology 72 (2) (2003) 179, Translated from Mikrobiologiya 72 (2) (2003) 212.
[17] M.J. Hernandez-Gayosso, G. Zavala-Olivares, N. Ruiz-Ordaz, R. Garcıa-Esquivel, J.L. Mora-Mendoza, Mater. Corros. 55 (9) (2004) 676.
[18] J. Jan-Roblero, J.M. Romero, M. Amaya, S. Le Borgne, Appl. Microbiol. Biotehnol. 64 (2004) 862.
[19] Zhu, X.Y J. Lubeck, J.J. Kilbane, Appl. Environ. Microbiol. 69 (2003) 5354.
[20] N. Muthukumar, S. Mohanan, S. Maruthamuthu, P. Subramanian, N. Palaniswamy, M. Raghavan, Electrochem. Commun. 5 (2003) 421.
[21] A. Rajasekar, S. Maruthamuthu, N. Muthukumar, S. Mohanan, P. Subramanian, N. Palaniswamy, Corros. Sci. 47 (2005) 257.
[22] S. Maruthamuthu, S. Mohanan, A. Rajasekar, N. Muthukumar, S. Ponmarippan, P. Subramanian, N. Palaniswamy, Ind. J. Chem. Tech. 12 (5) (2005) 567.
[23] W.H. Dickinson, Z. Lewandowski, Manganese biofouling of stainless steel: deposition rtes and influence on corrosion process, corrosion96, Paper No. 291, 1996.
[24] B.H. Oleson, R. Avci, Z. Lewandowski, Corr. Sci. 42 (2) (2000) 217.
[25] S.C. Dexter, S. Maruthamuthu, Response of passive alloys with n-type passive films to manganese in biofilm, Corrosion 2001 Paper No. 01256, p01256-1/01256-15, 2001.
[26] S. Maruthamuthu, S. Sathiyanarayanan, R. Palaniappan, N. Palaniswamy, Corrosion 2002, Paper No. 02468, 2002.
[27] J.G. Holt, N.R. Kreig, P.H.A. Sneath, J.T. Stanely, in: S.T. Williams (Ed.), Bergey's Manual of Determinative Bacteriology, Williams and Wilkins Publishers, Maryland, 1994.
[28] A. Rajasekar, S. Maruthamuthu, N. Palaniswamy, A. Rajendran, Microbiol. Res., in press.
[29] K.H. Nealson, The manganese-oxidizing bacteria, in: A. Balows, H.G. Truper, M. Dworkin, W. Harder, K.H. Schleifer (Eds.), The Prokaryotes, second ed., vol. 3, Springer-Verlag, New York, 1992, pp. 2310–2320.

[30] F.M. Ausubel, R. Brent, R.E. Kingston, D.D. Moore, J.G. Seidman, K.E. Struhl, Current protocols in molecular biology. Unit 24, Wiley, New York, 1988.
[31] W.G. Weisburg, S.M. Barns, D.A. Pelletier, D.J. Lane, J. Bacteriol. 173 (1991) 697.
[32] S.F. Altschul, G. Warren, W. Miller, E.W. Myers, D.J. Lipman, J. Mol. Biol. 215 (1990) 403.
[33] E. Rodriguez de Schiapparelli, B.R. de Meybaum, Mater. Perform. 19 (10) (1980) 47.
[34] B. Gerdes, R. Brinkmeyer, G. Dieckmann, E. Helmke, FEMS Microbiol. Ecol. 53 (1) (2005) 129.
[35] C. Calvo, F.L. Toledo, J. Gonzalez-Lopez, J. Biotech. 109 (2004) 255.
[36] J.Y. Richard, T.M. Vogel, Int. Biodeterio. Biodeg. 44 (1999) 93.
[37] N.Y. Frederic Chaillan, A.L. Flèche, E. Bury, Y. Phantavong, P. Grimont, A. Saliot, J. Oudot, Res. Microbiol. 155 (2004) 587.
[38] C. Fu, J. Zheng, J. Zhao, W. Xu, Corros. Sci. 43 (5) (2001) 881.
[39] S. Seal, K. Sapre, A. Kale, V. Desai, M. Gopal, P. Jepson, Corros. Sci. 42 (9) (2000) 1623.
[40] E. Miranda-Tello, M.-L. Fardeau, L. Fernández, F. Ramírez, J.-L. Cayol, P. Thomas, J.-L. Garcia, B. Ollivier, Anaerobe 9 (2003) 97–103.
[41] Bethencourtb, F.J. Botanab, M.J. Canob, J.M. Sánchez-Amayab, A. Corzoc, J. Garca de Lomasc, M.L. Fardeaua, B. Ollivera, Corro. Sci. 48 (9) (2006) 2417.
[42] L.G. Whyte, J. Hawari, E. Zhou, L. Bourbonniere, W.E. Inniss, C.W. Greer, Appl. Environ. Microbiol. 64 (1998) 2578.
[43] J.B. Van Beilen, M.G. Wubbolts, W.E. Witholt, Biodegradation 5 (1994) 161.
[44] R.W. Traxler, W.L. Flannery, Mechanism of hydrocarbon degradation, in: H.A. Walters, J. Elphick (Eds.), Biodeterioration of Materials, Microbiological and Allied Aspects, Elsevier publishing Co. Ltd., Amsterdam, 1968, pp. 44–53.
[45] F.M. Bento, G.E. Englert, C.C. Gaylarde, I.L. Muller, Mater. Corros. 55 (8) (2004) 577.
[46] K.H. Nealson, R.A. Rosson, C.R. Myers, Mechanisms of oxidation and reduction of manganese, in: T.J. Beveridge, R.J. Doyle (Eds.), Metal Ions and Bacteria, Wiley-Interscience, New York, 1989, pp. 383–411.
[47] David G. Kehres, Michael E. Maguie, FEMS Microb. Rev. (2003) 263.
[48] P. Linhardt, Biodegradation 8 (1997) 201.
[49] J.G. Jones, in: K.C. Marshall (Ed.), Iron Transformation by Fresh Water Bacteria in Advances in Microbial Ecology, Plenum, NY, 1986, p. 149.
[50] S.W. Borenstein, Mater. Perform. 27 (1988) 62.
[51] A.K. Tiller, in: Electrochemical Aspects of Microbial Corrosion, The Metals Society, London, 1983, pp. 54–65.
[52] R. Jeffery, R.E. Melchers, Corros. Sci. 45 (2003) 693.